

Department of Mathematics and Statistics

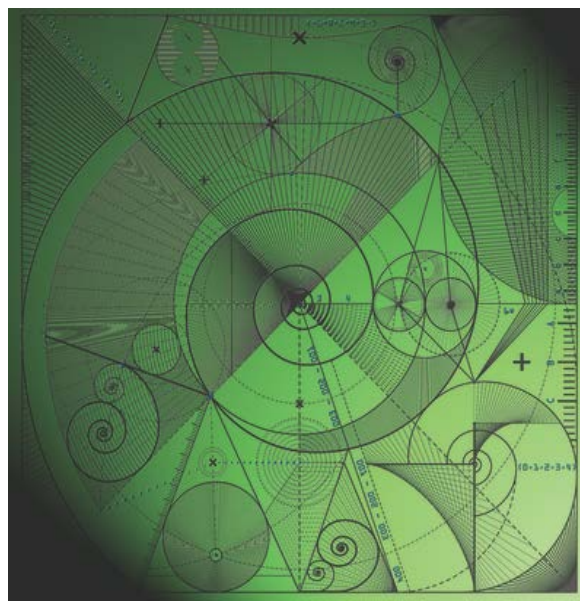
Preprint MPCS-2019-10

6 December 2019

A moving-mesh finite-difference method for segregated two-phase competition-diffusion

by

M.J. Baines and K. Christou



A moving-mesh finite-difference method for segregated two-phase competition-diffusion

M.J.Baines and K.Christou

Department of Mathematics and Statistics,
University of Reading, P.O.Box 220, Reading, RG6 6AX, UK

Abstract

A moving-mesh finite-difference solution of a Lotka-Volterra competition-diffusion model of theoretical ecology is described in which the competition is sufficiently strong to spatially segregate the two populations, leading to a two-phase problem with coupling conditions at the moving interface. The moving mesh approach preserves the identities of the two species in space and time, so that the parameters always refer to the correct population. The model is implemented numerically with a variety of parameter combinations illustrating how the populations evolve through time.

1 Introduction

We apply a moving mesh finite difference method based on conservation [4, 6] to a problem in population dynamics. A Lotka-Volterra competition model is considered that describes a two-phase segregated reaction-diffusion system with a high competition limit such that the species are completely spatially segregated and only interact using an interface condition [3, 5, 6].

It is shown in [2, 3] that where the competition is strong enough to spatially segregate the two populations the Lotka-Volterra system can be reduced to a form similar to a Stefan problem in physics [1]. The two major differences between the Stefan model and the Lotka-Volterra model are firstly, that there are additional logistic growth terms in the Lotka-Volterra model and

secondly, there is a parameter in the Lotka-Volterra model of the interface condition (the equivalent of the latent heat coefficient of the Stefan problem) which is set equal to zero. Unlike the Stefan problem, one species does not transform into another, which means that the competition system has an interface condition that specifies the interface velocity only implicitly.

A moving-mesh approach is an effective way to model this system because unlike fixed mesh descriptions it provides a framework for keeping particular mesh nodes attached to particular species rather than particular parts of space, and the dynamics for any given location are automatically those of the correct species.

We use the Lotka-Volterra model described by Hilhorst *et al.* in [3] approximated by the moving-mesh finite-difference method (MMFDM) of [4].

2 The Lotka-Volterra system

The Lotka-Volterra system is the two-component reaction-diffusion system

$$\frac{\partial u_1}{\partial t} = \delta_1 \frac{\partial^2 u_1}{\partial x^2} + f(u_1, u_2)u_1 \quad x \in R_1(t), \quad t > 0 \quad (1)$$

$$\frac{\partial u_2}{\partial t} = \delta_2 \frac{\partial^2 u_2}{\partial x^2} + g(u_1, u_2)u_2 \quad x \in R_2(t) \quad t > 0 \quad (2)$$

where $u_1(x, t)$ and $u_2(x, t)$ are the population densities of two competing species in abutting regions $R_1(t)$ and $R_2(t)$, the parameters δ_1, δ_2 are constant diffusion coefficients, and

$$f(u_1, u_2) = r_1 \left(1 - \frac{u_1 + K_1 u_2}{k_1} \right)$$

$$g(u_1, u_2) = r_2 \left(1 - \frac{u_2 + K_2 u_1}{k_2} \right).$$

are reaction terms in which K_1, K_2 are species-specific competition rates, k_1, k_2 are the carrying capacities of the species, and r_1, r_2 are reproductive rate parameters.

In [3] it is demonstrated that for two species completely segregated the reaction terms can be reduced to

$$f(u_1, u_2) = r_1(1 - u_1/k_1)$$

$$g(u_1, u_2) = r_2(1 - u_2/k_2).$$

so that equations (1) and (2) become

$$\frac{\partial u_1}{\partial t} = \delta_1 \frac{\partial^2 u_1}{\partial x^2} + \left\{ r_1 \left(1 - \frac{u_1}{k_1} \right) \right\} u_1 \quad x \in R_1(t), \quad t > 0 \quad (3)$$

$$\frac{\partial u_2}{\partial t} = \delta_2 \frac{\partial^2 u_2}{\partial x^2} + \left\{ r_2 \left(1 - \frac{u_2}{k_2} \right) \right\} u_2 \quad x \in R_2(t) \quad t > 0 \quad (4)$$

The resulting system represents the limit in which the carrying capacities K_1, K_2 values are very large, i.e. the competition rate is high enough that the two species cannot coexist in space and interact only through the interface boundary.

Initial conditions on u_1 and u_2 are selected such that one species is in growth and the other in decline. These are shown in figure (1).

Zero Neumann boundary conditions $\partial u_1/\partial x = 0$ and $\partial u_2/\partial x = 0$ are applied at fixed external boundaries away from the interface.

2.1 The interface conditions

At the interface between the two species there is a condition in [3] that gives the relationship between their fluxes. In essence, the species both flow into the interface and annihilate each other in a ratio determined by the competition coefficient μ . This condition is given as

$$\mu \delta_1 \frac{\partial u_1}{\partial x} = -\delta_2 \frac{\partial u_2}{\partial x} \quad (5)$$

where $\mu = K_2/K_1$ is the interspecies competition rate. Because the annihilation is complete we also have zero Dirichlet conditions $u_1 = u_2 = 0$ at the interface.

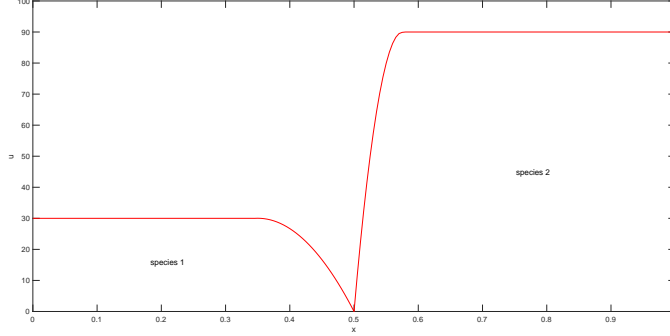


Figure 1: Initial conditions for the competition system, with population density u_1 of species 1 (on the left) and u_2 of species 2 (on the right). The interface node has zero population and must always satisfy the interface condition.

3 The MMFDM conservation method

3.1 A relative conservation principle

Define the total population of species p as

$$\theta_p(t) = \int_{R_p(t)} u_p(x, t) dx$$

($p = 1, 2$). Then by Leibnitz' Integral Rule,

$$\dot{\theta}_p = \frac{d\theta_p}{dt} = \frac{d}{dt} \int_{R_p(t)} u_p(x, t) dx = \int_{R_p(t)} \frac{\partial u_p}{\partial t} dx + [u_p v_p]_{R_p(t)}$$

The final term vanishes by the boundary and interface conditions, so

$$\dot{\theta}_p = \int_{R_p(t)} \frac{\partial u_p}{\partial t} dx \quad (p = 1, 2).$$

From (3) and (4),

$$\dot{\theta}_p = \int_{R_p(t)} \left(\delta_p \frac{\partial^2 u_p}{\partial x^2} + \left\{ r_p \left(1 - \frac{u_p}{k_p} \right) \right\} u_p \right) dx \quad (p = 1, 2) \quad (6)$$

which can be integrated in time to give θ_p .

We now suppose that population *fractions* $c(\Omega_p)$ in each moving subdomain $\Omega_p(t)$ are independent of time, so that $\theta_p(t)$ and $u_p(x, t)$ satisfy the *relative* conservation principle

$$\frac{1}{\theta_p(t)} \int_{\Omega_p(t)} u_p(x, t) dx = c(\Omega_p), \quad (p = 1, 2), \quad (7)$$

Since the population fractions $c(\Omega_p)$ are constant in time, they are determined by the conditions at the initial time t^0 , i.e.

$$c(\Omega_p) = \frac{1}{\theta_p(t^0)} \int_{R_p(t^0)} u_p(x, t^0) dx$$

Writing (7) as

$$\int_{\Omega_p(t)} u_p(x, t) dx = c(\Omega_p)\theta_p(t), \quad (p = 1, 2). \quad (8)$$

and differentiating the left hand side of (8) with respect to time using Leibnitz Integral Rule,

$$\frac{d}{dt} \left[\int_{\Omega_p(t)} u_p(x, t) dx \right] = \int_{\Omega_p(t)} \left(\frac{\partial u_p}{\partial t} + \frac{\partial}{\partial x}(u_p v_p) \right) dx, \quad (p = 1, 2)$$

where v_p is the velocity of points of the domain. Therefore, by (8), given the population fractions $c(\Omega_p)$, the velocity v_p and rate of change of the total mass $\dot{\theta}_p$ satisfy the equations

$$c(\Omega_p)\dot{\theta}_p - \int_{\Omega_p(t)} \frac{\partial}{\partial x}(u_p v_p) dx = \int_{\Omega_p(t)} \frac{\partial u_p}{\partial t} dx, \quad (p = 1, 2),$$

where the $\dot{\theta}_p$ are given by (3) or (4), giving

$$c(\Omega_p)\dot{\theta}_p - [u_p v_p]_{\Omega_p(t)} = \delta_p \left[\frac{\partial u_p}{\partial x} \right]_{\Omega_p(t)} + r_p \int_{\Omega_p(t)} u_p(x, t) \left(1 - \frac{u_p(x, t)}{k_p} \right) dx, \quad (9)$$

We let the subdomains $\Omega_1(t)$ in the region $R_1(t)$ consist of the interval $(a, x(t))$ where a is a fixed boundary and $x(t)$ is any point in the region $R_1(t)$. Similarly the subdomains $\Omega_2(t)$ in the region $R_2(t)$ consist of the

interval $(x(t), b)$ where b is a fixed boundary and $x(t)$ is any point in the region $R_2(t)$.

The boundary conditions at the external boundaries a and b are $\partial u_1/\partial x = \partial u_2/\partial x = 0$, and also $v_1 = v_2 = 0$ because the boundaries are fixed. Together with the condition that $u_1 = u_2 = 0$ at the interface boundary, equations (9) for the velocities v_1 and v_2 and the rates of change of the total mass $\dot{\theta}_1$ and $\dot{\theta}_2$ become

$$c_1(x)\dot{\theta}_1 - (u_1 v_1)|_{x(t)} = \delta_1 \left. \frac{\partial u_1}{\partial x} \right|_{x(t)} + r_1 \int_a^{x(t)} u_1(x, t) \left(1 - \frac{u_1(x, t)}{k_1} \right) dx \quad (10)$$

and

$$c_2(x)\dot{\theta}_2 + (u_2 v_2)|_{x(t)} = -\delta_2 \left. \frac{\partial u_2}{\partial x} \right|_{x(t)} + r_2 \int_{x(t)}^b u_2(x, t) \left(1 - \frac{u_2(x, t)}{k_2} \right) dx \quad (11)$$

respectively, where

$$\theta_1 = \int_0^{x_m(t)} u(x, t) dx, \quad \theta_2 = \int_{x_m(t)}^1 u(x, t) dx$$

and

$$c_1(x) = \frac{1}{\theta_1(t)} \int_0^{x(t)} u(x, t) dx, \quad c_2(x) = \frac{1}{\theta_2(t)} \int_{x(t)}^1 u(x, t) dx$$

From (6),

$$\dot{\theta}_1 = \delta_1 \left. \frac{\partial u_1}{\partial x} \right|_{x_m(t)} + r_1 \int_a^{x_m(t)} u_1(x, t) \left(1 - \frac{u_1(x, t)}{k_1} \right) dx \quad (12)$$

and

$$\dot{\theta}_2 = -\delta_2 \left. \frac{\partial u_2}{\partial x} \right|_{x_m(t)} + r_2 \int_{x_m(t)}^b u_2(x, t) \left(1 - \frac{u_2(x, t)}{k_2} \right) dx \quad (13)$$

3.2 The interface condition

Since the population density $u = 0$ at the interface and the population densities either side of the interface are positive, the density function is 'V' shaped at the interface.

From [3] the interface condition is given by (5). Whilst the interface velocity is not given explicitly by (5) this equation does determine the location of the interface implicitly. Thus, if we know $\partial u/\partial x$ adjacent to the interface in each region we may use the condition that $u = 0$ at the interface to infer an interface position such that the values of $\delta_p \partial u_p/\partial x$ either side of the interface are in the ratio $-\mu$.

We now describe a finite difference numerical method for the solution of the problem.

4 Numerical solution

Let the domain (a, b) be $(0, 1)$. At time level $t = t^n$ define time-dependent mesh points

$$0 = x_0 < x_1^n < \dots < x_{m-1}^n < x_m^n < x_{m+1}^n < \dots < x_N^n < x_{N+1}^n = 1$$

where x_m^n is the node at the moving interface, and let u_i^n , ($0 \leq i \leq N+1$), approximate $u(x, t)$ by u_i^n at these points.

The total mass approximations $\theta_1^n \approx \theta_1(t)$ and $\theta_2^n \approx \theta_2(t)$ of (12) and (13) are estimated by the composite trapezium rule

$$\theta_1^n = \sum_{i=1}^m \frac{1}{2} (u_{i-1} + u_i) (x_i - x_{i-1}), \quad \theta_2^n = \sum_{i=m}^N \frac{1}{2} (u_i + u_{i+1}) (x_{i+1} - x_i), \quad (14)$$

and the constant-in-time relative masses $c_{1,i}$ and $c_{2,i}$ in the interval (x_{i-1}^n, x_i^n) by

$$c_{1,i} = \frac{1}{\theta_1} \frac{1}{2} (u_{i-1}^0 + u_i^0) (x_i^0 - x_{i-1}^0), \quad (0 \leq i < m-1), \quad (15)$$

$$c_{2,i} = \frac{1}{\theta_2} \frac{1}{2} (u_i^0 + u_{i+1}^0) (x_{i+1}^0 - x_i^0), \quad (m+1 < i \leq N+1), \quad (16)$$

at the initial time $t = t^0$.

For the initial conditions we take the x_i^0 to be equally spaced and the u_i^0 pointwise from the initial function

$$\begin{aligned}
u(x, 0) &= 30, & (0 \leq x \leq 0.34) \\
u(x, 0) &= (x - 0.2)(0.5 - x) \times 170 \times 7.85, & (0.35 \leq x \leq 0.5) \\
u(x, 0) &= 0, & (x = 0.51) \\
u(x, 0) &= (x - 0.65)(0.5 - x) \times 170 \times 94, & (0.52 \leq x \leq 0.58) \\
u(x, 0) &= 90, & (0.59 \leq x \leq 1)
\end{aligned}$$

chosen to resemble the one in [2] (see figure 1).

4.1 Rates of change of the total populations

The rates of change of the total populations $\dot{\theta}_1, \dot{\theta}_2$ of (6) are approximated by composite trapezium rules, in region 1,

$$\begin{aligned}
\dot{\theta}_1 &= \delta_1 \left(\frac{u_m^n - u_{m-1}^n}{x_m^n - x_{m-1}^n} \right) \\
&+ r_1 \sum_{i=1}^m \frac{1}{2} \left\{ u_{i-1}^n \left(1 - \frac{u_{i-1}^n}{k_1} \right) + u_i^n \left(1 - \frac{u_i^n}{k_1} \right) \right\} (x_i - x_{i-1}) \quad (17)
\end{aligned}$$

from (12), and in region 2,

$$\begin{aligned}
\dot{\theta}_2 &= -\delta_2 \left(\frac{u_{m+1}^n - u_m^n}{x_{m+1}^n - x_m^n} \right) \\
&+ r_2 \sum_{i=m}^N \frac{1}{2} \left\{ u_i^n \left(1 - \frac{u_i^n}{k_2} \right) + u_{i+1}^n \left(1 - \frac{u_{i+1}^n}{k_2} \right) \right\} (x_{i+1} - x_i) \quad (18)
\end{aligned}$$

from (13).

4.2 Approximating the velocities

From (10), using the composite trapezium rule, the velocity v_i^n in region 1 satisfies,

$$c_{1,i} \dot{\theta}_1^n + u_i^n v_i^n = \delta_1 \left. \frac{\partial u}{\partial x} \right|_m^i$$

$$+r_1 \sum_{j=2}^i \frac{1}{2} \left\{ u_{j-1}^n \left(1 - \frac{u_{j-1}^n}{k_1} \right) + u_j^n \left(1 - \frac{u_j^n}{k_1} \right) \right\} (x_j - x_{j-1}), \quad (1 < i < m-1),$$

where we have taken the subdomain Ω_1^n to be the interval (x^n, x_m^n) . Similarly, from (11), the velocity v_2^n in region 2 satisfies

$$c_{2,i} \dot{\theta}_2^n + u_i^n v_i^n = -\delta_2 \left. \frac{\partial u}{\partial x} \right|_m^i$$

$$+r_2 \sum_{j=i}^N \frac{1}{2} \left\{ u_j^n \left(1 - \frac{u_j^n}{k_2} \right) + u_{j+1}^n \left(1 - \frac{u_{j+1}^n}{k_2} \right) \right\} (x_{j+1} - x_j), \quad (m+1 < i < N).$$

where we have taken the subdomain Ω_2^n to be the interval (x_m^n, x^n) .

4.3 Time-stepping

We adopt an explicit Euler time-stepping approach. Given the u_i , we update the total masses θ_p from the equation $\dot{\theta}_p = d\theta_p/dt$, ($p = 1, 2$) using (17) and (18) by

$$\theta_p^{n+1} = \theta_p^n + \Delta t \dot{\theta}_p^n \quad (19)$$

($p = 1, 2$), where Δt is the time step, and the mesh points x_i^n are updated from the equation $dx_i/dt = v_i$ by

$$x_i^{n+1} = x_i^n + \Delta t v_i^n \quad (i \neq m), \quad (20)$$

The updates are first-order accurate in time and subject to limitations on the time step to preserve node ordering.

Note that in case of a fixed mesh there is the following well-known sufficient condition on a time step Δt in the explicit scheme to prevent the u_i^{n+1} (and hence the local mass in an interval) going negative,

$$\frac{\delta_p \Delta t}{(\Delta x_{min})^2} \leq \frac{1}{2}, \quad (p = 1, 2) \quad (21)$$

Here we take (21) as a guide for a safe time step in the moving mesh case.

4.4 The population densities

In order to determine the approximate population densities u_i at the new time step $t = t^{n+1}$ from the θ_p^{n+1} and x_i^{n+1} we approximate the relative conservation principle (7) as

$$\frac{1}{\theta_p}(x_{i+1}^{n+1} - x_{i-1}^{n+1})u_i^{n+1} = \bar{c}_{p,i} \quad (p = 1, 2), \quad (22)$$

where from (15) and (16) the constants

$$\bar{c}_{p,i} = \frac{1}{\theta_p^0}(x_{i+1}^0 - x_{i-1}^0)u_i^0 \quad (p = 1, 2), \quad (23)$$

are independent of time.

Thus, once the x_i^{n+1} have been found, in region 1

$$u_i^{n+1} = \frac{\bar{c}_{1,i}\theta_1^{n+1}}{(x_{i+1}^{n+1} - x_i^{n+1})}, \quad (0 \leq i \leq m-2), \quad (24)$$

and in region 2

$$u_i^{n+1} = \frac{\bar{c}_{2,i}\theta_2^{n+1}}{(x_i^{n+1} - x_{i-1}^{n+1})} \quad (m+1 \leq i \leq N+1). \quad (25)$$

while $u_m^{n+1} = 0$ from the interface condition.

Note that the values of $u_{m\pm 1}^{n+1}$ determined by (22) depend on x_m^{n+1} , which is not yet known at t^{n+1} . This value can however be found using the one-sided approximations

$$u_{m-1}^{n+1} = \frac{c_1\theta_1}{\frac{1}{2}(x_{m-1}^{n+1} - x_{m-2}^{n+1})}, \quad u_{m+1}^{n+1} = \frac{c_2\theta_2}{\frac{1}{2}(x_{m+2}^{n+1} - x_{m+1}^{n+1})}$$

where from (15) and (16))

$$c_1 = \frac{1}{2}u_{m-1}^0(x_{m-1}^0 - x_{m-2}^0), \quad c_2 = \frac{1}{2}u_{m+1}^0(x_{m+2}^0 - x_{m+1}^0)$$

4.4.1 Approximating the interface

The interface condition (5) is approximated by

$$\mu\delta_1 \frac{u_m - u_{m-1}}{x_m - x_{m-1}} = -\delta_2 \frac{u_{m+1} - u_m}{x_{m+1} - x_m}, \quad (26)$$

where the subscript m denotes the interface node and the $x_{m\pm 1}, u_{m\pm 1}$ are adjacent node positions and solution values. Since $u_m = 0$, from (26) an approximation to the position of the interface node x_m^{n+1} in terms of adjacent nodal values at $m \pm 1$ is

$$x_m^{n+1} = \left(\frac{\mu\delta_1 u_{m-1}^{n+1} x_{m+1}^{n+1} + \delta_2 u_{m+1}^{n+1} x_{m-1}^{n+1}}{\mu\delta_1 u_{m-1}^{n+1} + \delta_2 u_{m+1}^{n+1}} \right). \quad (27)$$

Thus, once the other x_i^{n+1}, u_i^{n+1} have been updated, x_m^{n+1} can be found from (27).

4.5 Algorithm

In summary, the moving mesh finite difference solution of the competition-diffusion problem given by equations (3) and (4) with the interface condition (5) on the moving mesh in 1-D is given by the following algorithm.

From the initial mesh and the initial condition compute the initial values $\theta_p(0)$, ($p = 1, 2$) of the total populations of the species from (14) and the values of the relative masses $c_{p,i}$ and $\bar{c}_{p,i}$ from (15), (16) and (23).

Then for each time step:

1. Find the rates of change $\dot{\theta}_1, \dot{\theta}_2$ of the total masses from (17) and (18),
2. Calculate the nodal velocities v_i from (10) and (11),
3. Update θ_1 and θ_2 from $\dot{\theta}_1$ and $\dot{\theta}_2$ using the explicit Euler scheme (19),
4. Generate the nodal values x_i at the next time-step from the v_i using the explicit Euler scheme (20),
5. Update the population densities u_i at the next time level in each region from (24) and (25),
6. Update the new position of the interface node x_m at the next time level from (27).

5 Results

We find that the model is stable and robust. Even using the explicit Euler integration scheme we observe minimal oscillations affecting the smoothness of the results. in [1].

5.1 A parameter choice

In the body of work concerning Lotka-Volterra equations there is a vast range of parameter values in use because there are so many varied but suitable examples of the type of competition that are described here. We select a conservatively representative set of parameters, chosen to demonstrate some of the behaviour that this model is able to describe.

For the first example we choose a set of parameters that favour species 1, namely $\delta_1 = \delta_2 = 0.01$, $k_1 = k_2 = 100$, $r_1 = r_2 = 1$ and $\mu = 3$. In this case we see an increasing interface velocity in the initial stages (figure 2), followed by a change in direction where the interface velocity is approximately constant (figure 3). As we approach the annihilation of species 2, the interface velocity increases again due to the low mass of species 2 affecting its ability to grow. We see the interface increase in velocity after a slower initial phase where both species are experiencing population growth (figure 4). The interface accelerates as we approach an annihilation event. The movement of the interface is shown in figure 5.

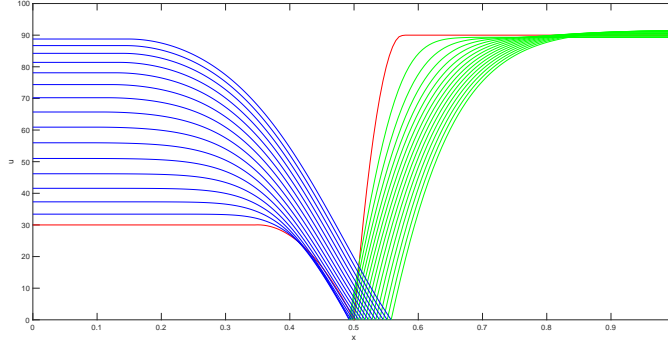


Figure 2: Result of competition model at $t = 1.5$. Here we use $\delta_1 = \delta_2 = 0.01$, $k_1 = k_2 = 100$, $r_1 = r_2 = 1$ and $\mu = 3$. We run the model with a time step of 0.00001 for 150000 iterations and plot the results every 0.01. We see the internal dynamics of the species driving the population densities and interface fluxes, and the position of the interface responding to those fluxes. The domain is $0 < x < 1$. The initial conditions are shown in red, with species 1 in blue and species 2 in green.

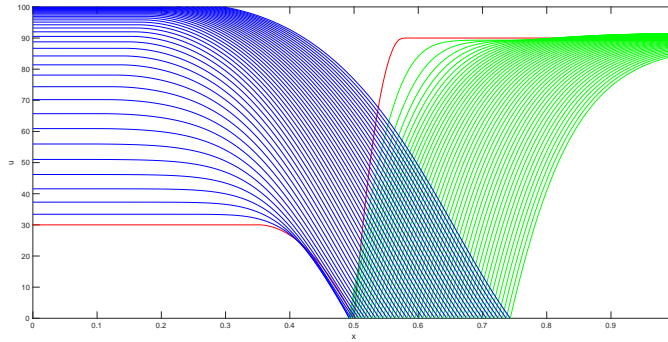


Figure 3: Result of competition model at $t = 4.5$. Here we use $\delta_1 = \delta_2 = 0.01$, $k_1 = k_2 = 100$, $r_1 = r_2 = 1$ and $\mu = 3$. We run the model with a time step of 0.00001 for 450000 iterations and plot the results every 0.01. The interface continues to evolve and the masses of the species are now limited by the respective carrying capacities. The domain is $0 < x < 1$. The initial conditions are shown in red, with species 1 in blue and species 2 in green.

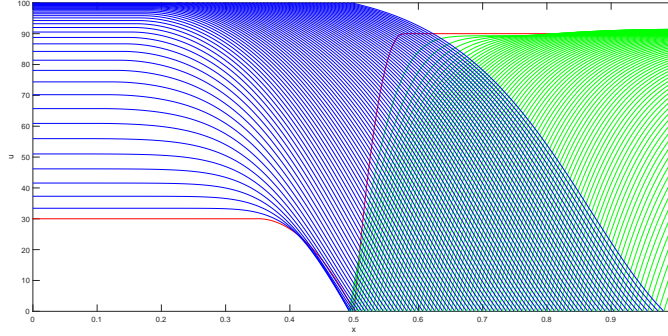


Figure 4: Result of competition model at $t = 8$. Here we use $\delta_1 = \delta_2 = 0.01$, $k_1 = k_2 = 100$, $r_1 = r_2 = 1$ and $\mu = 3$. We run the model with a time step of 0.00001 for 800000 iterations and plot the results every 0.01. We observe that whilst species 2 initially grew in mass, it will now be wiped out by competition with species 1. The domain is $0 < x < 1$. The initial conditions are shown in red, with species 1 in blue and species 2 in green.

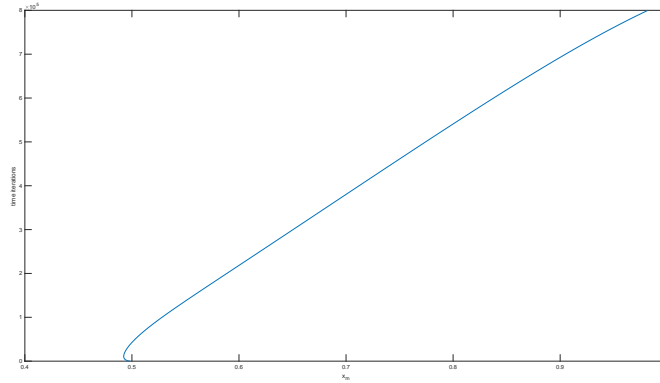


Figure 5: Movement of the interface position x_m against time for the competition model with parameters $\delta_1 = \delta_2 = 0.01$, $k_1 = k_2 = 100$, $r_1 = r_2 = 1$ and $\mu = 3$. We run the model with a time step of 0.00001 for 800000 iterations. We see the interface velocity accelerate as we approach an annihilation event.

5.2 Other parameter choices

5.2.1 Carrying capacities

We now investigate alternative parameter choices. We restrict the growth of species 1 by lowering its carrying capacity and observe that in this scenario neither species is dominant, even though all the competition and diffusion characteristics are unchanged. Here we use $\delta_1 = \delta_2 = 0.01$, $k_1 = 50$, $k_2 = 150$, $r_1 = r_2 = 1$ and $\lambda = 3$. With these differently chosen carrying capacities we find the interface position is approximately steady and the two species are in balance. This scenario is shown in Figure 6.

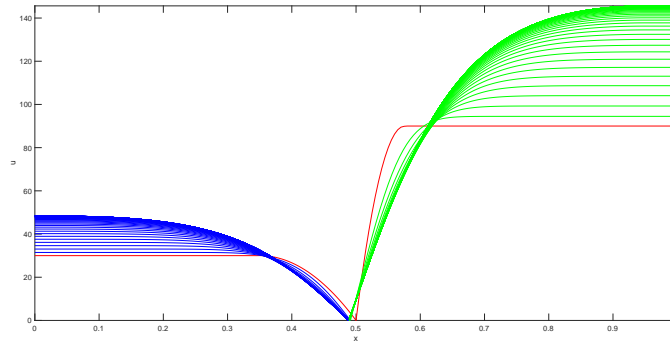


Figure 6: Result of competition model at $t = 9$, considering the effect of altered carrying capacities. Here we use $\delta_1 = \delta_2 = 0.01$, $k_1 = 50$, $k_2 = 150$, $r_1 = r_2 = 1$ and $\mu = 3$. We run the model with a time step of 0.00001 for 150000 iterations and plot the results every 0.01. The figure shows the rapid territorial gains. The initial conditions are shown in red, with species 1 in blue and species 2 in green. The domain is $0 < x < 1$.

5.2.2 Diffusion characteristics

Alternatively we may adjust the diffusion characteristics of the system. By allowing species 2 to diffuse at a higher rate, we observe that species 2 is able to make territorial gains due to this property alone (figure 7). Here we use $\delta_1 = 0.01, \delta_2 = 0.05, k_1 = k_2 = 100, r_1 = r_2 = 1$ and $\mu = 3$. Due to the growth characteristics we can see interesting temporal effects. Here the interface velocity has actually reversed directions as the system changes from diffusion dominated to growth dominated. We observe that species 2 is able to make territory gains initially due to its high diffusion rate, even though the competition rate is unaltered. However, as time goes on, the growth and competition characteristics become increasingly important. We see species 1 becoming more dominant over time, so that the interface velocity actually reverses direction.

Figure 8 shows the evolution of the system at $t = 11$, and figure 9 shows the movement of the interface with the direction reversal.

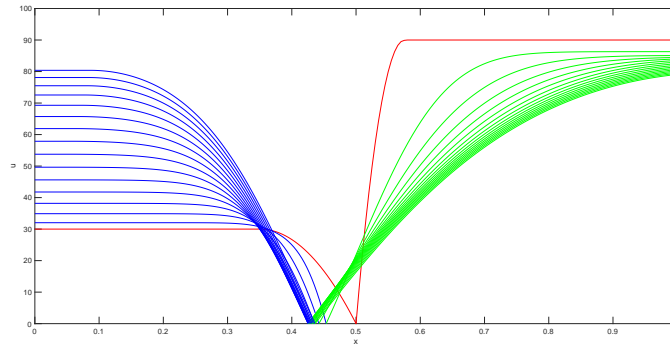


Figure 7: Result of competition model at $t = 1.5$, considering the effect of an increased diffusion rate for species 2. Here we use $\delta_1 = 0.01, \delta_2 = 0.05, k_1 = k_2 = 100, r_1 = r_2 = 1$ and $\mu = 3$. We run the model with a time step of 0.00001 for 150000 iterations, and plot the results every 0.01. The figure shows the rapid territorial gains of species 2 over species 1 due to its high diffusion rate. The initial conditions are shown in red, with species 1 in blue and species 2 in green. The domain is $0 < x < 1$.

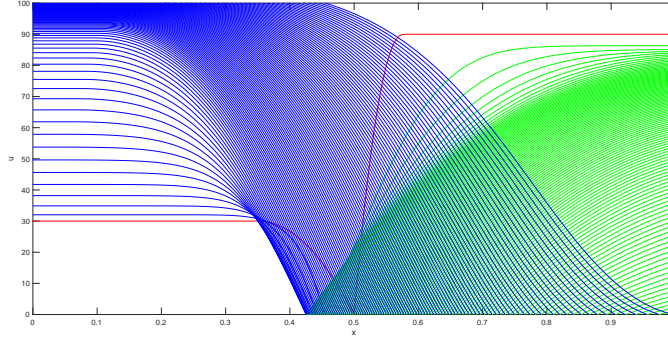


Figure 8: Result of competition model at $t = 11$, considering the effect of an increased diffusion rate for species 2. Here we use $\delta_1 = 0.01, \delta_2 = 0.05, k_1 = k_2 = 100, r_1 = r_2 = 1$ and $\mu = 3$. We run the model with a time step of 0.00001 for 1100000 iterations, and plot the results every 0.01. We see that the initial diffusion-driven gains by species 2 are reversed, and that the overall growth characteristics are dominating so that species 1 is gaining territory. The initial conditions are shown in red, with species 1 in blue and species 2 in green. The domain is $0 < x < 1$.

These illustrations give confidence that the model is likely to be able to satisfy the requirements of modelling a wide variety of competition systems. It is stable to a large choice of set-up parameters and is able to produce complex behaviours without problems.

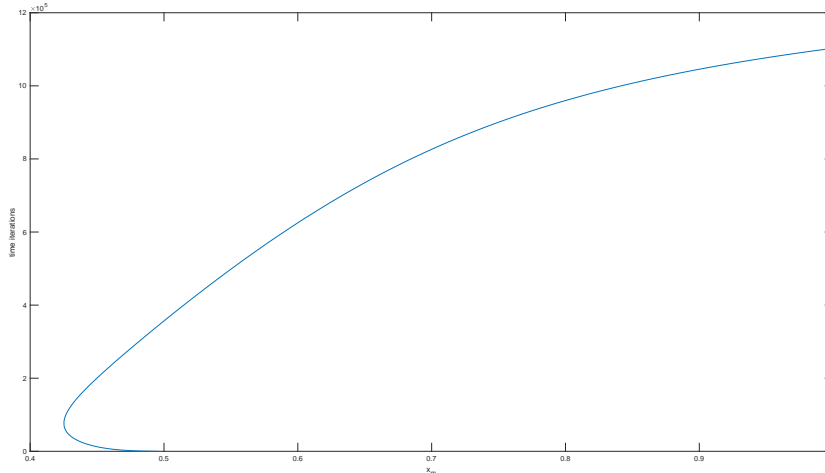


Figure 9: Position of interface x_m against time, showing interface movement for the competition model at up to $t = 11$, considering the effect of an increased diffusion rate for species 2. Here we use $\delta_1 = 0.01, \delta_2 = 0.05, k_1 = k_2 = 100, r_1 = r_2 = 1$ and $\mu = 3$. We run the model with a time step of 0.00001 for 1100000 iterations. Due to the growth characteristics we can see interesting temporal effects. Here the interface velocity has actually reversed direction as the system changes from diffusion-dominated to growth-dominated.

6 Summary

In this paper we have applied the moving mesh finite difference method based on a conservation principle (MMFDM) of [4] to a two-phase Lotka-Volterra competition system with a high competition limit [3], such that the species are completely spatially segregated and interact solely through an interface condition based on this limit.

In section 2 the model is described in detail. In section 3 the MMFDM implemented. In section 4 numerics. In section 5 illustrations are given for a variety of parameter combinations, observing the various behaviours that dominate as the species evolve through time.

For a set of parameters that favour species 1 we see an increasing interface velocity in the initial stages followed by a long steady phase where the interface velocity is approximately constant. Although the population of species

2 initially grows it is eventually wiped out by the competition with species 1. As the annihilation of species 2 is approached, the interface velocity increases again. The interface continues to evolve and the populations of the species are then limited by the respective carrying capacities. This is due to the low population of species 2 affecting its ability to grow.

If the growth of species 1 is restricted by lowering its carrying capacity we observe that neither species is dominant, even though all the competition and diffusion characteristics are unchanged. Increasing the diffusion rate for species 2, this species is able to make initial territorial gains, even though the competition rate is unaltered. However, as time goes on, growth and competition characteristics become increasingly important and species 1 becomes more dominant, so the interface velocity reverses direction.

A natural extension is to two dimensions along the lines described in [1], a first attempt appearing in reference [5] which foundered on stability issues. In further work it would be interesting to compare the behaviour of the model against an empirical data set. The model lends itself to alterations to the logistic terms and changes to parameters without the need for any further development. The aim should be to understand the requirements from both a mathematical and quantitative perspective.

Acknowledgements: The authors wish to acknowledge the work of Watkins [5] (see also [6]) using finite elements in the motivation for this work.

References

- [1] M.J. BAINES, M.E. HUBBARD, P.K. JIMACK, AND R. MAHMOUD, A moving-mesh finite element method and its application to the numerical solution of phase-change problems), *Commun in Comput.Phys.*, 6, pp. 595-624 (2009).
- [2] CROOKS, E, DANCER, E, HILHORST, D AND MIMURA, M AND NINOMIYA, H, *Spatial segregation limit of a competition-diffusion system with Dirichlet boundary conditions*, *Nonlinear Analysis: Real World Applications*, (2004).
- [3] HILHORST, D AND MIMURA, M AND SCHÄTZLE, R *Vanishing latent heat limit in a Stefan-like problem arising in biology*, *Nonlinear analysis: real world applications*, 4, pp.261-285, 2003.

- [4] T.E. LEE, M.J. BAINES, AND S. LANGDON, *A finite difference moving mesh method based on conservation for moving boundary problems*, J. Comp. Appl. Math, 288, pp.1-17 (2015).
- [5] A.R.WATKINS, *A Moving Mesh Finite Element Method and its Application to Population Dynamics*, PhD thesis, University of Reading, UK (2017),
- [6] A.R.WATKINS AND M.J.BAINES, *A two-phase moving mesh finite element model of segregated competition-diffusion preprint MPCS-2018-07*, Department of Mathematics and Statistics, University of Reading, UK (2017).